JCTC Journal of Chemical Theory and Computation

Effects of Discrete Charge Clustering in Simulations of Charged Interfaces

John M. A. Grime* and Malek O. Khan

Department of Physical and Analytical Chemistry, Physical Chemistry, Uppsala University, Uppsala, Sweden

Received January 7, 2010

Abstract: A system of counterions between charged surfaces is investigated, with the surfaces represented by uniform charged planes and three different arrangements of discrete surface charges - an equispaced grid and two different clustered arrangements. The behaviors of a series of systems with identical net surface charge density are examined, with particular emphasis placed on the long ranged corrections via the method of "charged slabs" and the effects of the simulation cell size. Marked differences are observed in counterion distributions and the osmotic pressure dependent on the particular representation of the charged surfaces; the uniformly charged surfaces and equispaced grids of discrete charge behave in a broadly similar manner, but the clustered systems display a pronounced decrease in osmotic pressure as the simulation size is increased. The influence of the long ranged correction is shown to be minimal for all but the very smallest of system sizes.

1. Introduction

The study of charged interfaces is of interest in a variety of diverse fields, for example electrochemistry,[1] pharmaceutical research, [2] and membrane biology.[3−5] Perhaps the most common traditional models of such interfaces use the Poisson−Boltzmann approximation for the treatment of electrostatic interactions, a "mean field" approach which predicts a purely repulsive interaction between like-charged interfaces. The absence of counterion correlations in such a model fail to predict the existence of attractive regimes,[6,7] however, and hence can be of less general applicability where length scales are on the order of nanometres. Such microscopic effects may be significant in the study of a variety of biochemical processes such as vesicle/liposome aggregation and fusion[4] as well as for colloidal stability.[7] Charged interfaces are conventionally approximated in simulation as uniformly charged surfaces,[6−10] but at the microscopic level surface charge exists as discrete packets. It is therefore of interest to examine any differences in the energy and pressure produced in model systems featuring different representations of an identical net surface charge density, and it is reasonable to assume that the ability of the discrete charges to colocate into clusters will affect the surface−surface interactions as well as the counterion distributions. In order to treat these effects accurately, it is essential to correctly treat the long-range electrostatics.

Naji and Podgornik[11] have demonstrated how two surfaces, with a quenched charge disorder, have an attractive component to the force between the two surfaces. Mamasakhlisov et al.[12] extended this field theory approach and state that partial annealing of mobile wall ions, which move on a slower time scale than the counterions, enlarges the attractive interwall force. Using both a field-theoretical approach and Monte Carlo simulations, Fleck and Netz,[13,14] have shown that surface charge disorder leads to counterions being more attracted to the surface in comparison with ordered surface charges. Studying a slightly different problem, Naydenov et al.[15] show theoretically that two different charged wall species can form finite domains and that the resulting domains depend both on short-range attractive forces and electrostatics (via the salt concentration).

We present certain differences in the properties of a system of counterions between like-charged surfaces, modeled using Monte Carlo simulations of both uniformly charged surfaces and surfaces bearing discrete charges at various levels of surface charge clustering. Particular attention is paid to the energy of a counterion as a function of the z coordinate (perpendicular to the charged surfaces) and the osmotic

* Corresponding author e-mail: john.grime@fki.uu.se.

10.1021/ct100009m
Published on Web 09/13/2010

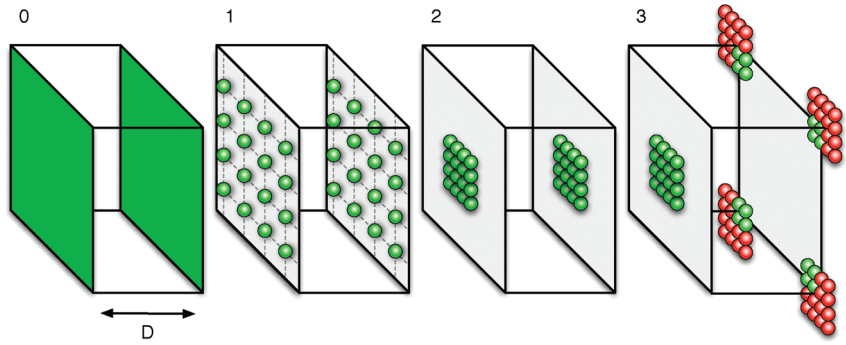

Figure 1. Illustration of the four system types studied here. From left to right; uniformly charged planes (system 0, planes shown in green), equidistantly spaced discrete wall charges (system 1, wall charges shown in green), clustered discrete wall charges directly opposite (system 2), clustered discrete wall charges with maximum separation between clusters on opposing walls (system 3, periodic wall charges shown in red to emphasize periodic boundaries). Counterions not shown.

pressure with respect to the potential system size dependence for a commonly used simulation technique.

Four types of systems are considered, as shown in Figure 1. Briefly, these consist of two parallel planes of uniform surface density σ (system 0), a lattice arrangement of equispaced discrete wall charges (system 1) and two arrangements of discrete wall charges condensed into square clusters positioned directly opposite one another on the two walls (system 3) and with the maximum spacing possible in the simulation cell (system 3).

2. Method

Monte Carlo simulations for counterions contained between a pair of uniformly charged surfaces are well established.[6−10] The energy of the system is described as a combination of interionic effects (including Coulomb interactions and a hard sphere potential), ion-wall interactions, and a long ranged correction to account for the relatively slow decay of the electrostatic potential and the limited system size

$$U = U_{\mathrm{q}} + U_{\mathrm{HS}} + U_{\mathrm{w}} + U_{\mathrm{LRC}} \tag{1}$$

Here the interionic potentials U_{q} and U_{HS} are sums over the N interacting particles

$$U_{\mathrm{q}} = \sum_{i=1}^{N-1} \sum_{j=i+1}^{N} \frac{q_i q_j e^2}{4\pi\varepsilon_0\varepsilon_1 r_{ij}} \tag{2}$$

$$U_{\mathrm{HS}}(i,j) = \sum_{i=1}^{N-1} \sum_{j=i+1}^{N} \begin{cases} \infty & \text{where } r_{ij} < r_{\mathrm{HS}} \\ 0 & \text{otherwise} \end{cases} \tag{3}$$

with q_1 and q_2 being the charges on the ions (in elementary charge units, e), and ε_1 is the permittivity of the medium relative to that of vacuum (ε_0). The separation between particles i and j is r_{ij}, and any overlap of the hard spheres surrounding the charges (i.e. $r_{ij} < r_{\mathrm{HS}}$) produces an infinite energy penalty to ensure such a situation does not occur during simulation. We consider only single-valence ions with a hard sphere radius of 1 Å. The choice of $\varepsilon_1 = 78.5$ is made to approximate an aqueous solution, giving the Bjerrum length, $l_B = e^2/(4\pi e_0 e_1 k_B T) \approx 7.1$ Å at the simulated temperature of 300 K.

Ion-wall interactions are simply those of a point charge and an infinite plane of uniform surface charge density σ

$$U_{\mathrm{w}} = \sum_{i=1}^{N} -\frac{\sigma q_i e}{2\varepsilon_0\varepsilon_1}\left(\left|\frac{D}{2} + z_i\right| + \left|\frac{D}{2} - z_i\right|\right) \tag{4}$$

Note that here we assume the plane at $z = 0$ bisects the two charged walls; hence, the origin lies in the center of the simulation cell, and $z = \pm(D)/2$ are the positions of the charged wall planes. The energy of the interaction between the two walls themselves is constant during simulation and is therefore ignored for the purposes of the Monte Carlo procedure. Where discretely charged walls are present, the energy expression becomes somewhat simpler - the counterion/wall interactions are already considered explicitly via the Coulomb pair potential (in the minimum image convention) and its long ranged correction, and hence U_{w} above is ignored.

To ensure a flat plane of closest approach for the counterions, we add an excluded region of volume extending to twice the ion hard sphere radius in front of each wall. This also provides identical accessible volume to the counterions for comparable systems with either uniform of discretely charged walls.

Finally, the long ranged correction to the electrostatic energy is performed under the "charged planes" formulation of Valleau et al.[7] All discrete charges in the system (counterions and discrete wall charges, where present) contribute to an average charge density profile on the axis perpendicular to the wall planes. This average distribution forms the charge density on a series of charged slabs (infinite in the plane parallel to the walls) arranged in a stack between the wall planes. The long ranged correction to the electrostatic energy for a discrete charge is then the interaction with this series of infinite slabs (cf. eq 4) minus the interaction of the charge with the finite regions of each slab which lie inside the simulation cell

$$U_{\mathrm{LRC}} = \sum_{i=1}^{N} \sum_{s=1}^{S} -\frac{\sigma q_i e}{2\varepsilon_0\varepsilon_1}\left(|s_i - z_i| + \frac{W}{2\pi} f(|s_i - z_i|/W)\right) \tag{5}$$

Table 1. Charged Wall Dimension *W* as a Function of *L* for the Systems Studied

L	1	2	3	4	5	6	7	8	9
W, Å	12.66	25.32	37.97	50.63	63.29	75.95	88.60	101.26	113.92

where W is the x dimension of the simulation cell on the wall plane (assumed to be square, so x and y dimensions are both W) and

$$f(z) = 4\ln\left(\frac{0.5 + r_1}{r_2}\right) - 4z\left(\sin^{-1}\left[\frac{r_2^2 + 0.5 \times r_1}{0.5 \times r_2 + r_1 r_2}\right] + \tan^{-1}\left[\frac{1}{2z} - \frac{\pi}{2}\right]\right) \quad (6)$$

with

$$r_1 = (0.5 + z^2)^{1/2} \quad (7)$$

$$r_2 = (0.25 + z^2)^{1/2} \quad (8)$$

Using this procedure, the average charge distribution normal to the wall planes (and hence the long ranged contribution to the electrostatic energy) may be generated self-consistently.

We adopt the convention of describing the wall charges with the parameter L; for example, $L = 4$ describes an set of 4×4 wall charges which lie on the wall plane. By changing L, we can investigate the size dependence of the systems at a constant total surface charge density provided we ensure appropriate simulation cell dimensions and enforce charge neutrality with a suitable number of counterions (with the net counterion concentration also held constant across simulations). A series of systems with $1 \leq L \leq 9$ is considered, and for the case of system type 0 (see Figure 1) the walls are represented by uniformly charged planes of the appropriate area which ensures charge neutrality and dimensions identical to a discretely charged system of equal L and σ. The wall dimensions in the simulation cell which correspond to the studied values of L for $\sigma = 0.1$ Cm^{-2} are listed in Table 1. In all cases, the separation D between the planes of closest approach for a counterion to the charged walls is 15 Å, more than twice the Bjerrum length for a system of this nature.

The osmotic pressure is measured at the midplane of the system,[6,7,16] where the counterion concentration varies slowly. Such an approach helps to reduce uncertainty in the kinetic contribution to the pressure, which may be poorly defined in the regions of rapidly changing concentration adjacent to the charged planes; such an artifact can lead to difficulties where the pressure is evaluated according to, for example, the contact theorem.[6,17] We calculate the pressure according to the formulation of Valleau et al.,[7] with certain changes; Valleau et al. simplified the expression by noting that the charge on each plane exactly balanced, on average, the charge from the counterions in one-half of the simulation cell, and hence certain components of the pressure cancel for uniformly charged walls. This is not the case for systems with discrete wall charges, and hence we use the full pressure expression with no simplifying assumptions in each simulation. This treatment was confirmed to reproduce the values of the simplified expression[7] for systems with uniformly charged walls. The long ranged correction to the electrostatic energy for each system studied was generated using 2.5×10^7 Monte Carlo cycles, with a cycle defined as n attempted moves of a randomly selected counterion, with n being the number of counterions in the system. All data used herein were produced from an additional 2.5×10^7 Monte Carlo cycle.

3. Results and Discussion

3.1. Uniformly Charged Walls. We first examine the size dependence of certain observables in systems with uniformly charged walls. The counterion charge density profiles and mean total energy of a counterion as a function of the z coordinate are shown in Figure 2, where we observe that the results are effectively independent of system size. As the energy contribution from an infinite, uniformly charged plane and a point charge is linear in distance (eq 4), and the counterions are contained between symmetrical surfaces with identical surface charge density, this charge distribution is effectively a result of the counterion correlations as the energy due to the walls is constant for all counterion positions. *Any* value of σ will produce the same counterion charge distributions given the same systems size and counterion concentration, although such systems are unphysical where a net charge exists.

The total osmotic pressure, however, shows a strong size dependence for small L as can be seen in Figure 2. The value of P is very much lower for $L = 1$ compared to $L = 2$ ($\approx$460 mM vs $\approx$560 mM), for example. As L increases, we observe a fast convergence onto a stable value of $P \approx 575$ mM. This demonstrates the robust nature of such a representation, even at relatively small systems sizes.

3.2. Discrete Wall Charges on an Equispaced Grid. Although uniformly charged surfaces are both convenient for analytical theory and computationally efficient in models of charged interfaces, at the microscopic level such an interface features discrete packets of charge from embedded ions or partial charges in the wall material. We therefore examine the effects of replacing the uniformly charged surfaces with regular grids of discrete charges (see system 1, Figure 1). All the parameters are otherwise identical to those considered previously.

Figure 3 shows the counterion charge distribution for a series of systems with discretely charged walls of $1 \leq L \leq 9$. Somewhat surprisingly the results are very comparable, even for small L, with slight differences becoming apparent only in the regions very close to the charged walls. The results are similar to those of the uniformly charged walls (see Figure 2) albeit with slightly higher concentrations immediately adjacent to the wall which reflects the stronger attraction of the counterions to the discrete wall charges at close ranges. This difference is rather subtle, in agreement with the findings of Fleck and Netz[13,14] who noted that, where wall charge exists in regularly spaced packets, the effects on the counterion distribution - specifically the tendency for counterions to aggregate closer to the charged

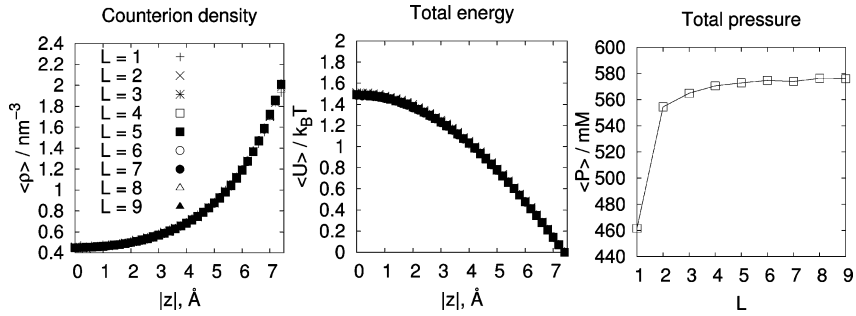

Figure 2. Counterion distributions perpendicular to the interfaces, total energy of a counterion as a function of z position, and total pressure for the systems with uniformly charged walls (system 0, see Figure 1). Energy given as excess over that at the plane of closest approach to the wall, $|z| = 7.5$ Å. Histogram resolution is 5 bins per Å, with the data point plotted at the center of each histogram bin. Error bars are too small to be shown clearly.

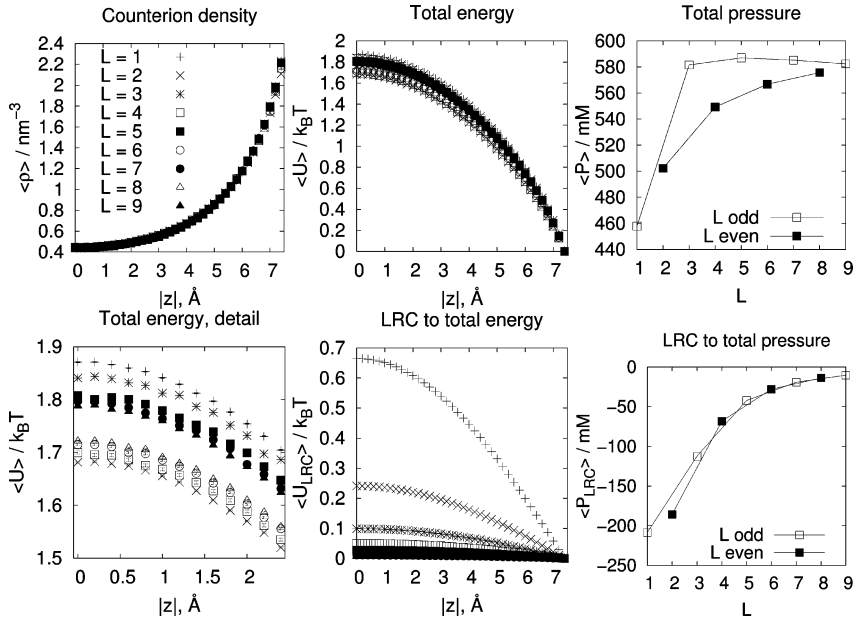

Figure 3. Simulation results for systems with equidistantly spaced discrete wall charges (system 1, see Figure 1). Data are as in Figure 2, with the addition of a detailed plot of the counterion energy in the midplane region and the long ranged contributions to the total energy and pressure. Energies are given as excess over that at the plane of closest approach to the wall, $|z| = 7.5$ Å. Error bars are too small to be shown clearly.

wall - is much reduced compared to systems with disordered arrangements of wall charge.

As the interactions between the counterions and the wall charges are modeled using a combination of a short ranged Coulomb potential (in the minimum image convention) and a long ranged correction to the electrostatic energy, care must be taken to avoid asymmetry due to different numbers of discrete wall charges on the x and y plane either side of a counterion. Where L is an even number, we can encounter pronounced asymmetry in the number of wall charges which are explicitly considered on either side of the counterion on the x and y axes. In the limit of large L this effect will vanish, but for relatively small systems the effects can be significant. Where L is an odd number, however, we expect this asymmetry to be reduced as the counterion can preferentially locate next to any of the discrete wall charges, and the odd L allows the minimum image convention to provide an equal number of wall charges in both directions on the x and y axes.

This effect can be seen in the total energy of a counterion as a function of its z position (Figure 3), where there are two main groups of results; systems where L is odd, and systems where L is even. Wall charge arrangements with odd L appear to slightly overestimate the mean energy of a counterion as a function of z coordinate, whereas the even L systems appear to slightly underestimate the mean energy. As L increases, the mean energy for both odd and even L converges onto an intermediate value.

The long ranged correction to the total energy of a counterion between discretely charged walls as a function of z position is also shown in Figure 3. As expected, smaller systems require a larger LRC - but the magnitude of this correction decays rapidly as L increases. For $L \geq 4$, the long ranged correction contributes, on average, less than 3% of the total energy as a function of counterion z position.

A similar pattern is seen in the osmotic pressure (Figure 3); here P appears to have effectively converged for odd values of $L \geq 3$, whereas convergence for even values of L

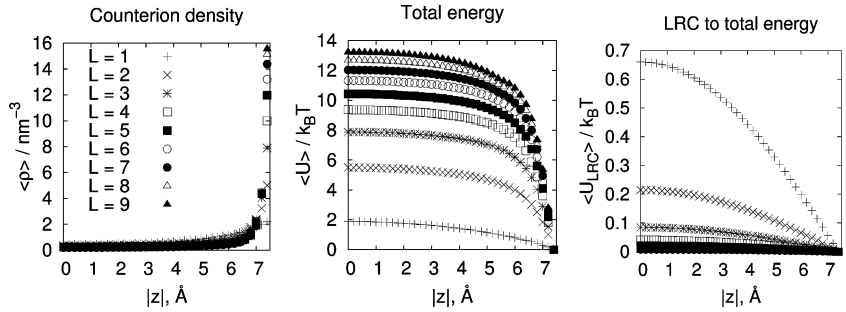

Figure 4. Charge distributions perpendicular to the interfaces, total energy of a counterion as a function of *z* position, and the contribution of the long ranged correction to the total energy for the systems with clustered discretely charged walls (system 2, see 1). Energy given as excess over that at the plane of closest approach to the wall, $|z| = 7.5$ Å. The simulation results for system 3 are almost indistinguishable from these data. Error bars are too small to be shown clearly.

requires a larger system. The long ranged correction to the pressure decays rapidly in L, as did the long ranged correction to the energy. The total pressure converges onto a value which is very similar to that of the uniformly charged walls (ca. 580 mM at $L = 9$).

3.3. Discrete Wall Charges and the Effects of Clustering. We have so far considered a charged interface as described by both a uniformly charged surface and a regular lattice of discrete charges. These models produce very comparable counterion distributions perpendicular to the interface, and there is rapid convergence onto similar pressure as L increases. However, not all surfaces can be adequately described in these terms; an interface with a particular mean σ may consist of pockets of relatively high and low surface charge density. Interfaces of equal net σ as modeled by uniform charge densities and regularly spaced discrete charges can produce qualitatively and quantitatively different counterion concentration profiles, for example in the case of rodlike counterions,[17] and the variable clustering of discrete surface charges may further affect the energy and pressure in a given system.

A quantitative discussion of the surface charge clustering found in various experimental systems is problematic due to the difficulties of directly measuring these aspects of an interface. Although there is experimental evidence to suggest the presence of charged domain formation in, for example, lipid membrane systems,[18−21] quantitative analysis of the size of the charged domains formed has proven to be difficult. Even though the existence of such domains is well recognized in vitro, there remains some debate as to their presence for in vivo membrane systems.[21]

We now examine the extreme situation of discrete wall charges condensing into a single cluster with high local surface charge density but the same net σ and system composition as those discussed previously. The two model arrangements of clustered discrete surface charge are depicted in Figure 1 as systems 2 and 3, and here wall charges are staggered on the x and y axes with spacing equal to the impenetrable diameter of the wall charges (2 Å) to form square arrangements of clustered discrete charge.

For this aspect of the study, further attention is given to the effects of the long ranged electrostatic correction via the charged slabs method. As this correction is calculated from the average charge distribution in the system via the counterion concentration profiles, any significant changes to this distribution via clustering of the wall charges (with a subsequent shift in average counterion density) has the potential to affect the properties of the system. We therefore simulate each of systems 1, 2, and 3 (see Figure 1) using not only the LRC appropriate to the system itself but also the LRC of the other two discretely charged system types (of equal size and net σ) to examine the significance of the LRC.

We adopt the notation LRC_n to describe the long ranged correction from system n (see Figure 1). There are 9 sets of simulations performed, as each of the three arrangements of discrete wall charges are simulated using the three different long ranged corrections for every value of L.

The simulation results for system types 2 and 3 (see Figure 1) are extremely similar, and hence only the counterion density profiles, energy, and LRC for system 2 are plotted in Figure 4. Both clustered systems display very different properties when compared to the systems with uniformly charged walls (Figure 2) and unclustered discretely charged walls (Figure 3). As L increases, we are no longer simply adding additional repeating sections to the simulation cell as was the case for the uniformly charged and unclustered discretely charged wall systems. Instead, the models represent what are effectively different types of interface, which can be seen in the pronounced changes of the counterion density profiles and energy as L increases. This is readily explained in terms of the rapid increase in the local surface charge density of the clustered region of the walls relative to the expansion of the overall wall dimensions in the simulation cell; this effect is particularly noticeable for large L, where we observe a density of $\rho \geq 10$ e nm^{-3} adjacent to the clustered walls compared to $\rho \approx 2$ e nm^{-3} for the uniformly charged and unclustered discretely charged walls. Such behavior demonstrates the utility of measuring pressures at the midplane of the system, as the large changes in counterion concentration make techniques such as the contact theorem numerically problematic at the plane of closest approach to the charged surfaces.

In all cases, providing the LRC from a different discretely charged system of equal size and net σ does not noticeably alter the counterion charge distributions perpendicular to the charged walls, and nor is there a discernible effect on the energy of a counterion as a function of z (data not shown).

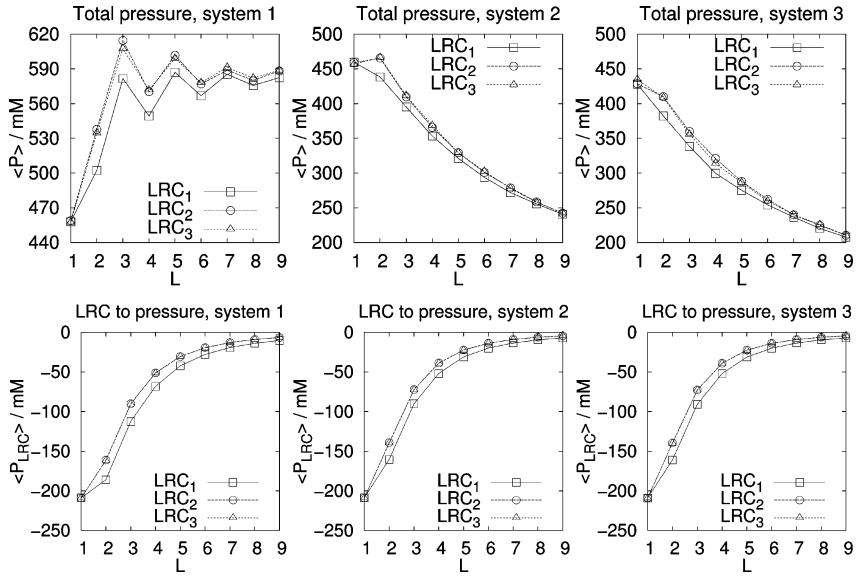

Figure 5. Total and long ranged contribution to P for the three discretely charged wall systems. Compare total pressure data for system 1 to Figure 3, where this pressure is separated into even and odd *L*. Error bars are too small to be shown clearly.

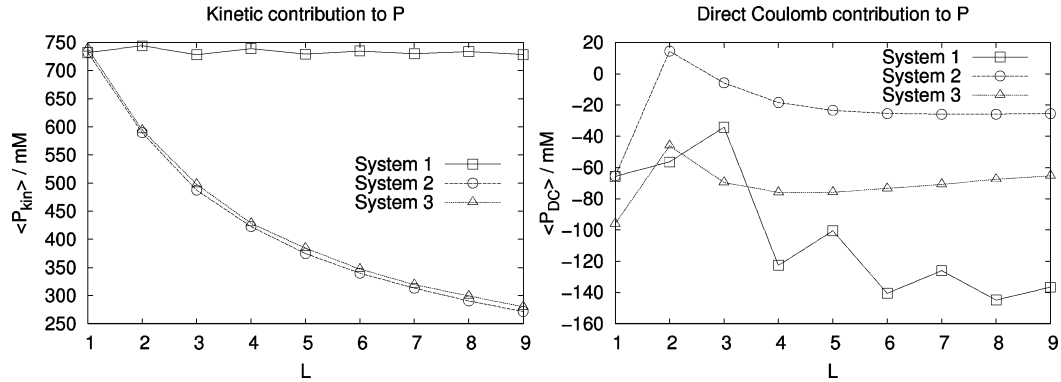

Figure 6. Individual components of the osmotic pressure for systems 1, 2, and 3 (Figure 1). In each case, the "native" long ranged correction appropriate to the system is used. Error bars are too small to be shown clearly.

Figure 5 displays the recorded pressures for systems 1, 2, and 3 for the values of *L* studied here. For system 1, where the wall charges are arranged on an equispaced grid, *P* quickly increases in *L* to values which oscillate around the approximate plateau value of *P* for the uniformly charged systems (Figure 2), with the magnitude of the oscillations decreasing as *L* increases. This effectively demonstrates the convergence of *P* onto a similar value to that of system 0, showing that these two representations are basically equivalent provided the system is sufficiently large (although this is not necessarily valid for high electrostatic coupling[16]). In systems 2 and 3, where the wall charges are densely clustered, *P* behaves in an entirely different manner - essentially *decreasing* as a function of *L*.

The completely different trend in *P* as a function of *L* for the clustered systems cannot be explained by the LRC to the pressure, which is seen to be very similar in each case (Figure 5). Figure 6 shows the kinetic and direct Coulomb contributions to the total pressure, and we observe that the reduction in *P* is largely a result of the marked decrease in the kinetic contribution to the osmotic pressure as a function of *L* in systems with clustered wall charges. This is an expected effect of the very large counterion concentrations in the vicinity of the clustered wall charges, with a conjugate depletion of counterions in the middle of the systems where the kinetic contribution to *P* is measured (compare, for example, the counterion densities in Figure 3 and Figure 4). Although the equispaced grid arrangement of wall charges in system 1 leads to a smaller direct Coulomb pressure contribution with increasing *L*, this reduction is small compared to the differences in kinetic pressure we see between system 1 and systems 2 and 3. For both the kinetic and direct Coulomb contributions to the osmotic pressure for system 1, we again see the characteristic oscillations, which decrease in magnitude with increasing *L*. The measured hard sphere contribution to the pressure is orders of magnitude smaller than the other contributions and hence is ignored in this discussion.

The total pressures measured for system 3 are consistently somewhat lower than those of system 2; again, the LRC contributions to the pressure are almost identical, and the answer may be found in Figure 6 where we see that although the kinetic contribution to *P* for system 3 is consistently slightly higher than that of system 2, the direct Coulomb pressure found in system 3 is markedly lower as the repulsion between like-charged wall ions on the opposing surfaces is

decreased as the distance between the clusters on the x, y plane increases. This produces a net P which is marginally lower for the systems with misaligned wall clusters compared to clusters which are positioned directly opposite one another.

4. Conclusion

Charged interfaces of a particular net surface charge density σ may be represented in models as uniformly charged planes, discretely charged walls with equidistant charge spacing, or walls with locally clustered discrete wall charges. Although the behaviors of the former two systems are known to differ under certain circumstances, here we show that the addition of local clustering of the discrete wall charges can itself change the nature of the system entirely via large differences in the counterion distributions and an enhanced sensitivity of the energy and osmotic pressure to the size of the simulation cell, even in the presence of long ranged corrections to the electrostatic energy.

The long ranged correction to the electrostatic energy and pressure become rapidly less significant as a fraction of the total energy and pressure as the system increases in size. We show that despite the sensitivity of the long ranged corrections used here to the average charge profile of the system, in many cases a precomputed charge distribution will suffice to reproduce the essential behaviors regardless of the level of wall charge clustering in the system used to precompute the long ranged correction and the actual system of interest.

Notably, we observe a trend of rapidly decreasing osmotic pressure as a function of system size for clustered arrangements of wall charges. The osmotic pressure for such clustered arrangements can be $\approx$1/3 of that measured from equidistantly spaced discrete wall charges or uniformly charged surfaces for the range of systems studied. We observe that these changes are largely the result of the electrostatic interaction within the simulation cell and that the influence of the long ranged corrections to the energy and pressure decay rapidly as a function of system size for the simulation methods used.

Acknowledgment. We acknowledge the high performance computational (and storage) capacity allocated through the Swedish National Infrastructure for Computing (SNIC) on resources at the National Supercomputer Centre (NSC), alongside the UPPMAX high performance computational resources provided by Uppsala University under Project SNIC s00109-20. M.O.K. also acknowledges an Ingvar Carlsson grant from The Swedish Foundation for Strategic Research.

References

(1) Piedade, J. A. P.; Mano, M.; de Lima, M. C. P.; Oretskaya, T. S.; Oliveira-Brett, A. M. *Biosens. Bioelectron.* **2004**, *20*, 975–984.

(2) Carla, M.; Cuomo, M.; Arcangeli, A.; Olivotto, M. *Biophys. J.* **1995**, *68*, 2615–2621.

(3) Düzgünes, N.; Nir, S.; Wilschut, J.; Bentz, J.; Newton, C.; Portis, A.; Papahadjopoulos, D. *J. Membr. Biol.* **1981**, *59*, 115–125.

(4) Ekerdt, R.; Papahadjopoulos, D. *Proc. Nat. Acad. Sci. U.S.A.* **1982**, *79*, 2273–2277.

(5) Evans, E.; Kukan, B. *Biophys. J.* **1983**, *44*, 255–260.

(6) Guldbrand, L.; Jönsson, B.; Wennerstrm, H.; Linse, P. *J. Chem. Phys.* **1984**, *80*, 2221–2228.

(7) Valleau, J. P.; Ivkov, R.; Torrie, G. M. *J. Chem. Phys.* **1991**, *95*, 2221–2228.

(8) Jönsson, B.; Wennerström, H.; Halle, B. *J. Phys. Chem.* **1980**, *84*, 2179–2185.

(9) Urbanija, J.; Bohinc, K.; Bellen, A.; Maset, S.; Iglič, A.; Kralj-Iglič, V.; Kumar, P. B. S. *J. Chem. Phys.* **2008**, *129*, 1051015–1011055.

(10) May, S.; Iglič, A.; Reščič, J.; Maset, S.; Bohinc, K. *J. Phys. Chem. B* **2008**, *112*, 1685–1692.

(11) Naji, A.; Podgornik, R. *Phys. Rev. E* **2010**, *72*, 041402−1−041402−11.

(12) Mamasakhlisov, Y. S.; Naji, A.; Podgornik, R. *J. Stat. Phys.* **2008**, *133*, 659–681.

(13) Fleck, C. C.; Netz, R. R. *Europhys. Lett.* **2005**, *70*, 341–347.

(14) Fleck, C. C.; Netz, R. R. *Eur. Phys. J. E* **2007**, *22*, 261–273.

(15) Naydenov, A.; Pincus, P. A.; Safran, S. A. *Langmuir* **2007**, *23*, 12016–12023.

(16) Khan, M. O.; Petris, S.; Chan, D. Y. C. *J. Chem. Phys.* **2005**, *122*, 1047051–1047057.

(17) Grime, J. M. A.; Khan, M. O.; Bohinc, K. *Langmuir* 2010In press.

(18) Huang, J.; Swanson, J. E.; Dibble, A. R. G.; Hinderliter, A. K.; Feigenson, G. W. *Biophys. J.* **1993**, *64*, 413–425.

(19) Hinderliter, A. K.; Huang, J.; Feingenson, G. W. *Biophys. J.* **1994**, *67*, 1906–1911.

(20) Ahn, T.; Yun, C.-H. *J. Biochem.* **1998**, *124*, 622–627.

(21) Allender, D. W.; Schick, M. *Biophys. J.* **2006**, *91*, 2928–2935.

CT100009M